# Perpendicular magnetic anisotropy and noncollinear magnetic structure in ultrathin Fe films on W(110)

M. Ślęzak,[1,*] T. Ślęzak,[1] K. Freindl,[2] W. Karaś,[1] N. Spiridis,[2] M. Zając,[3,†] A. I. Chumakov,[3] S. Stankov,[3,‡] R. Rüffer,[3] and J. Korecki[1,2]

[1]*Faculty of Physics and Applied Computer Science, AGH University of Science and Technology, al. Mickiewicza 30, 30-059 Kraków, Poland*

[2]*Jerzy Haber Institute of Catalysis and Surface Chemistry, Polish Academy of Sciences, Niezapominajek 8, Kraków, Poland*

[3]*European Synchrotron Radiation Facility, BP 220, 38043 Grenoble Cedex, France*

(Received 15 October 2012; revised manuscript received 11 January 2013; published 11 April 2013)

We used nuclear resonant scattering (NRS) of synchrotron radiation to investigate the details of the thickness-induced spin reorientation transition (SRT) in ultrathin epitaxial iron films on W(110), where the thicknesses of the films ranged from 1–5 monolayers. During growth, the magnetization of the Fe film, which was probed by the hyperfine magnetic field, changes from a noncollinear configuration with an out-of-plane magnetic component to the homogeneously magnetized state with the in-plane [1-10] easy direction. The fast acquisition of the experimental NRS spectra combined with the high sensitivity of this technique to the orientation of the hyperfine magnetic fields allowed us to study the magnetic evolution during SRT in detail. Our results reveal the complex character of this transition, which has been intensively studied in the past. The noncollinear magnetic structure appears in the system of the mono-, double-, and trilayer areas that coexist due to deviation from the layer-by-layer growth of iron on W(110). We also report the observation of out-of-plane magnetic anisotropy in the double-layer areas at temperatures as high as 300 K. By comparing the experimental results with density functional theory calculations, we conclude that surface magnetic moments are enhanced by 25%.

DOI: 10.1103/PhysRevB.87.134411 PACS number(s): 75.70.−i, 75.70.Ak, 75.70.Rf, 75.75.−c

## I. INTRODUCTION

The magnetic properties of nanoscale materials are currently of considerable scientific and technological interest. The complex magnetic structures that often occur in low-dimensional systems[1] present a challenge for the currently available experimental methods. Considerable research efforts have been focused on ultrathin iron films grown on the W(110) surface, which are considered to be the archetype of a 2-D ferromagnet.[2] These films have been studied using advanced scanning probe microscopy,[3] spin sensitive electron scattering techniques,[2] x-ray magnetic dichroism,[4] the magneto-optic Kerr effect (MOKE),[5] torsion oscillation magnetometry (TOM),[6] and $^{57}$Fe conversion electron Mössbauer spectroscopy (CEMS).[7,8]

The most interesting properties of Fe films grown on the W(110) surface have been observed in films that have thicknesses up to a few monolayers. The Fe monolayer (ML) on the W(110) surface is thermodynamically stable, unlike iron MLs grown on other substrates systems, such as Fe/Cu,[9] Fe/Ag,[10] and Fe/Au.[11] Due to the large misfit of 9.4% between the Fe and W lattices, the pseudomorphic ML (psML) is completed at a coverage of 0.82 ML, which is measured in units of one bulk Fe(110) ML. Concerning the magnetic order, the existence of noncollinear magnetic structures, e.g. spin spirals, have been theoretically predicted to occur on the unsupported Fe(110) ML.[12–14] However, when the strong spin-orbit coupling at the Fe/W(110) interface is considered, ferromagnetic ordering is energetically favored over the creation of spin spirals,[12] which is in agreement with experimental observations.[15] The magnetization of this ferromagnetic ML ($T_C = 230$ K, Ref. 2) is confined to the film plane with a pronounced twofold anisotropy, and the easy axis points along the [1-10] direction.[15]

When pseudomorphic Fe(110) sesquilayers (sesqui = one and a half) are prepared at room temperature (RT) on W(110), puzzling magnetic phenomena are observed. The striking sensitivity of the $T_C$ to the submonolayer coverages of Fe, Pd, Ag, and $O_2$ was reported by Weber *et al.*[16] for this thickness range. Elmers *et al.*[17] observed an unusual suppression of the remanent magnetic long-range order between 1.2 and 1.5 psML, whereas Skomski *et al.*[18] observed high coercivities on the order of 0.3 T at 140 K near 1.4 psML of coverage. It has been recognized that the nanomorphology of these films plays a crucial role in understanding their magnetic properties.[17,18] Such films are composed of ferromagnetic (superparamagnetic) double-layer (DL) islands that are surrounded by a ML sea, which becomes ferromagnetic below 222 K (Refs. 2 and 19). It has been reported[20] that the easy axis of the magnetic DL islands is perpendicular to the plane, whereas that of the ML sea points along the [1-10] in-plane direction. Upon adsorption of residual gases, the spin reorientation transition (SRT) to the (110) plane was observed in the DL areas.[21] The out-of-plane magnetic contrast in the DL areas, in a wide range of coverage, from isolated DL islands at 1.2 ML up to nearly closed DL films at 2.1 ML, was reported using low-temperature (15 K) spin-polarized scanning tunneling spectroscopy (SP-STS) by Kubetzka *et al.*[22] For small islands, which have a width of 2–3 nm, the authors observed that the magnetic out-of-plane contrast disappeared, and they interpreted this observation as the reorientation transition to the film plane, which was driven by the exchange coupling to the in-plane magnetized ML sea. It was shown that, in the top-most layer of the large DL islands, the local magnetization direction is inhomogeneous, with a gradual canting of the magnetic moment from the perpendicular direction in the center of the island towards an in-plane direction at the edges. For the continuous DL prepared at elevated temperature and thus containing dislocation lines,

 

the out-of-plane magnetized stripe domains were found at 15 K.[23]

To summarize this section, we would like to emphasize certain experimental limitations when studying magnetic properties at the nanoscale level. The SP-STS technique has a defined depth resolution because the sensitivity of this technique is strictly confined to the surface. The capabilities of this technique can also be influenced by the adsorption of residual gases, which may be significant, especially at low temperatures. Other methods, such as MOKE, TOM, and x-ray magnetic dichroism, integrate the magnetic properties over a large surface area or over all of the atoms of a particular element.[4–6] In this respect, CEMS[7,8] and, recently, grazing incidence nuclear resonant scattering (GI-NRS)[24] of synchrotron radiation are exceptional since, due to their selectivity resulting from the isotopic probe-layers concept, they enable studying magnetic properties with atomic depth resolution. Furthermore, the data acquisition time for GI-NRS is extremely short compared to other surface-sensitive techniques, especially CEMS, due to the high brilliance of third generation synchrotron radiation sources.

Notwithstanding the considerable progress that has been achieved in explaining the magnetic properties of ordered striped nanostructures that combine ML and DL structures,[25] a few questions concerning the magnetism of Fe/W(110) ultrathin films still remain unanswered: (1) What is the intrinsic (in the absence of effects caused by adsorption and magnetically isolated from the ML sea) magnetic structure of the DL islands? (2) Is the depth profile of the magnetization structure homogenous? (3) How does the magnetic structure depend on the size of the DL areas, and what is the magnetic state in the limit of the perfect (continuous) DL? To answer these questions, we undertook the present study of the magnetic properties of Fe/W(110) films in a relatively wide (1.0–5.2 ML) coverage range using the NRS technique. Room temperature was chosen for both the growth of Fe (above 1.0 psML) and the NRS measurements; therefore, the ML areas were in the paramagnetic state, and the coupling effects suggested in Ref. 22 could be avoided. Fast data acquisition, which is a characteristic for the GI-NRS method, enabled us to minimize the effects induced by the adsorption of residual gases on the evolution of the magnetic state of the iron films. Using a small coverage step of approximately 0.4 Å, the magnetic properties could be almost continuously monitored, beginning from the nucleation of small and separated DL islands, through the coexistence of the nearly closed DL and third atomic layer (AL) patches, to the thicker films. The local character of the magnetic information obtained by the NRS technique provided the possibility to answer the question about the magnetic structure homogeneity in the DL islands with atomic site sensitivity. However, the local magnetization is indirectly probed via the hyperfine magnetic field ($B_{hf}$), and for surfaces and interfaces, there is no simple relationship between $B_{hf}$ and the magnetic moments.[26] Therefore, to interpret the measured hyperfine magnetic field in terms of the magnetization profiles, we performed *ab initio* density functional theory (DFT) calculations, which revealed some trends in the relationships between the magnetic moment versus $B_{hf}$.

## II. EXPERIMENTAL DETAILS

A newly constructed, ultrahigh vacuum (UHV) system[27] at the nuclear resonance beamline[28] (ID18) at the European Synchrotron Radiation Facility (ESRF), Grenoble, enables state-of-the-art preparation and characterization of single crystalline surfaces and epitaxial films, and it is capable of evaporating several metals (including Fe isotopes). The unique feature of this system is a special chamber that permits diverse *in situ* GI-NRS experiments, either during or shortly after the deposition of $^{57}$Fe.

The geometry of the NRS experiment is schematically shown in Fig. 1. The scattering NRS UHV chamber (base pressure of $1 \times 10^{-10}$ Torr) was mounted on a Huber two-circle goniometer. Two large diameter beryllium UHV windows allowed the incident and scattered x-ray beams to access the sample and an avalanche photodiode (APD) detector array, respectively. The grazing incidence angle (∼3.8 mrad) geometry was optimized for the maximum count rate of the delayed quanta intensity. As shown in Fig. 1, $^{57}$Fe was deposited from a thermally heated vapor source onto a freshly cleaned W(110) crystal that was pre-aligned with respect to the x-ray beam. The structure of the samples was examined using low-energy electron diffraction (LEED) in a peripherally attached preparation/analysis chamber. Using a remote-operated shutter and a precise $^{57}$Fe flux monitor, the entire preparation process could be operated online from the control cabin without stopping the x-ray beam. Therefore, the time of the experiment was minimized, which ensured a clean preparation of the Fe films. It was also important to access the virgin magnetic states because, in contrast with most magnetic measurements, a magnetic field is not required for the NRS measurements.

The following preparation protocol was used. Because of the restricted nucleation of the layers, the first psML (1.64 Å) was deposited at 600 K to ensure its high continuity. At thicknesses exceeding 1 ML, the remainder of the film, to a total coverage of ∼10 Å, was deposited at RT at a rate of ∼0.12 Å/min, and all of the GI-NRS measurements were also performed at RT. In the following text, when the Fe thickness is provided for MLs, it is assumed that the initial two MLs are pseudomorphic and that the following layers have the density of bulk Fe(110). To avoid time-consuming sample adjustment after rotating the sample, two different samples were prepared for measuring the RT time spectra with the incident x-ray beam parallel to the [1-10] and the [001] in-plane crystallographic directions of the W(110)

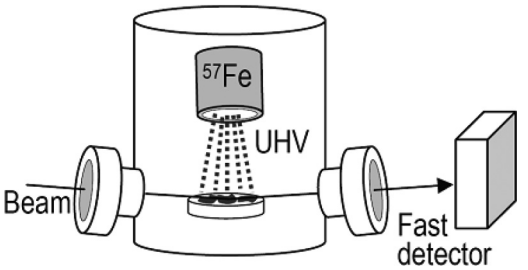


FIG. 1. Schematic of the UHV NRS scattering chamber at the nuclear resonance beamline (ID18) at the ESRF.

surface. The option of performing GI-NRS measurements for different sample orientations combined with the subsequent consistent fitting procedure during the analysis stage is an important contribution to the unambiguous determination of the magnetic structure. Additionally, the measurement procedure that enables the acquisition of the GI-NRS time spectra along with the film deposition makes the method fast enough to minimize the influence of the adsorption of residual gases that was discussed in Ref. 21. For a given direction of the incident x-ray beam, it was possible to complete the entire experimental run for the $^{57}$Fe films in the thickness range of 1.6 Å (1 ML) to 10 Å (step 0.4 Å) in ∼3 h, and the total residual gas exposure was approximately 1.0 Langmuir (L). The total residual gas exposure between two subsequent NRS measurements was approximately 0.25 and 0.05 L for the thinnest films, where the onset of magnetism was observed, and for the thickest films, respectively. Both exposure values are significantly lower than the critical exposure of 1 L that results in the out-of-plane to in-plane SRT in the DL areas, as reported by Durkop *et al.*[21] Furthermore, for the freshly grown Fe deposits, the total residual gas exposure during the evaporation and measurement processes reached only ∼0.12 L for the longest acquisition time (1200 s for 1.5 ML). Therefore, the effects of adsorption during each experimental step can be assumed to be negligible.

Complementary LEED and scanning tunneling microscopy (STM) measurements were performed in a separate UHV system to obtain information about the morphology of the films grown under specific conditions.

## III. NRS TECHNIQUE

The NRS[24] technique is a synchrotron radiation analogue of the Mössbauer spectroscopy (MS) technique in the sense that recoilless excitation (induced by the resonant x rays with an energy of 14.4 keV for $^{57}$Fe) of the nuclear energy levels, which split due to the hyperfine interactions, is involved. In this method, the hyperfine parameters can be derived from a characteristic beat pattern observed in the time evolution of the intensity of the nuclear resonant scattering (the so-called time spectrum). In the conventional MS methods, such as CEMS, the hyperfine interactions are measured via incoherent processes, in which the decay of the nuclei that are resonantly excited by $\gamma$ quanta occurs via resonance fluorescence or internal conversion. The resulting spectrum is the incoherent sum of single events. In contrast, the NRS signal, which is measured after the simultaneous excitation of an ensemble of nuclei by a pulse of synchrotron radiation, results from the coherent superposition of the probability amplitude for scattering from all of the nuclei of the ensemble. An extensive description of this method and its application is available in several review papers[29,30] and a comprehensive book.[24]

For films or surfaces, NRS is performed using a specular reflection geometry at grazing incidence, as shown in Fig. 2.

This technique has recently been demonstrated to be a powerful one specifically for studying noncollinear magnetic structures in single thin magnetic films[31] and multilayers.[32]

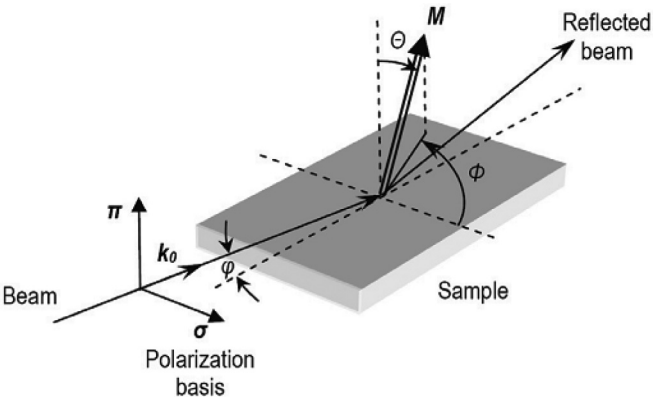


FIG. 2. (Reproduced after Ref. 24) Geometry of the GI-NRS experiment. The angles Θ and Φ provide the relative orientation of the incident synchrotron beam wave vector $\mathbf{k_0}$ to the magnetization $M$. Here, $\sigma$ and $\pi$ are the linear polarization basis vectors. The grazing angle $\varphi$ is typically a few milliradians.

The applicability of the GI-NRS technique for true *in situ* surface studies under UHV conditions has been demonstrated for epitaxial Fe nanostructures on a single crystalline tungsten substrate.[31,33]

In this paper, the measured NRS time spectra were fitted using the software package CONUSS[34] based on the dynamical theory of nuclear scattering. The fitting of NRS spectra is usually difficult if dynamic effects overlap with a complex hyperfine interaction pattern. However, in the present study, there are two circumstances that allowed this problem to be overcome. First, for the low coverage of the investigated Fe films, the effects of multiple scattering are negligible, and consequently, the so-called dynamical beats[24] do not appear in the measured time spectra, which results in a considerably more simplified fitting procedure compared to that for the thicker Fe films. Second, two independent measurements with the incoming radiation wave vector $\mathbf{k_0}$ parallel to the W[1-10] and W[001] directions were performed for each iron coverage, and the resulting sets that consisted of the two spectra were consistently fitted within a common model. This procedure, although complicated and time consuming, ensured that the physical information extracted from the NRS spectra was reliable and unambiguous.

Another problem is the interpretation of the magnetic hyperfine fields $B_{hf}$. In the majority of the theoretical literature data on Fe/W(110),[35,36] only the magnetic moments $\mu$ are treated, whereas the relationship between $B_{hf}$ and $\mu$ is not obvious, and especially for surfaces and interfaces, this relationship extends considerably beyond a simple proportionality.[37,38] Therefore, the elucidation of the experimental $B_{hf}$ data in terms of the local magnetization requires direct comparison with theoretical calculations. For this purpose, DFT calculations were performed using the WIEN2K code. The primary objective of the DFT calculations was to calculate the magnetic moments and the magnetic hyperfine fields of a double layer of Fe/W(110) simulated in a slab geometry by (2 ML Fe)/7 ML W(110)/(2 ML Fe). For a reference, calculations were also performed for 7 ML Fe(110) such that our results can be compared with the existing literature data on the Fe(110) surface.[37,39]

## IV. RESULTS—OVERVIEW OF THE MODEL

The analysis and interpretation of the measured NRS spectra were based on the AL model of Fe films considering deviation from the flat growth for the given preparation conditions. The first ML that was grown at elevated temperature is continuous,[40] whereas the subsequent layers are not, which can be concluded from previous studies and was also directly confirmed by STM observations. For example, the STM image in Fig. 3 reveals that, for the nominal coverage of 2.2 ML, four height levels are exposed, and this deviation from the ideal layer-by-layer growth mode leads to the coexistence of Fe ML, DL, trilayer (TL) and higher patches. Therefore, the number of atomic configurations in this RT grown real film is considerably greater than in the ideal flat film that consists of an integer number of ALs, in which the number of specific iron sites simply corresponds to the number of layers. In rough films, one has to consider all of the ALs in all of the Fe patches of different heights, which was considered during the interpretation of the NRS time spectra.

Figure 4 shows a selection of the fitted time spectra for $\mathbf{k_0}$ parallel to the [1-10] and [001] directions in the W(110) plane and the evolution of the magnetic structure derived from the best fits obtained with the software package CONUSS.[34] For a given coverage, the fits for both of the sample orientations were obtained with identical magnitudes (the numbers in Fig. 4 indicate the hyperfine fields in Teslas), orientations (arrows in Fig. 4), distributions of hyperfine parameters, and contributions of all components (represented by the areas of rectangles in Fig. 4). We do not present the derived isomer shifts (IS) and quadrupole splittings (QS) because they are not informative in the context of this paper. However, note that the magnitudes of QS and IS were maintained constant for both measured sample orientations. The in-plane angles between the hyperfine magnetic fields and $\mathbf{k_0}$ were fixed to 0° and 90° for $\mathbf{k_0}$ parallel to the [1-10] and [001], respectively, which is consistent with the [1-10] easy magnetization axis in this thickness range.[2]

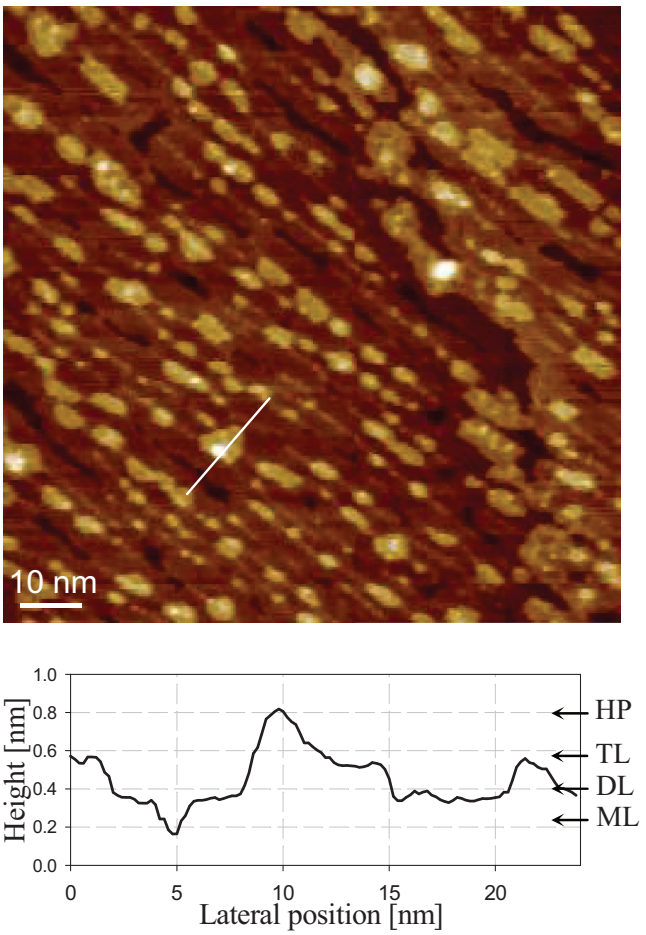


FIG. 3. (Color online) The STM image for the nominal coverage of 2.2 ML of Fe on W(110). Exemplary cross-sectional profile reveals four height levels exposed: ML, DL, and TL areas, as well as higher Fe patches (HP).

The most complex spectra were collected for the films with three or more exposed height levels. For example, for the nominal coverage range of 1.75 to 2.40 ML, up to eight sites were considered, which differentiated the Fe atoms in the first AL on tungsten of the ML, DL, TL patches, and then the Fe atoms in the second AL of the DL and TL patches, and finally, the Fe atoms in the third (surface) layer of the TL patches. Additionally, two types of DL patches were distinguished with individual magnetic hyperfine field values for each layer.

The model is simplified for lower and higher coverages. This simplification occurs for the thinnest films because of the disappearance of the subsequent layers, and for the lowest studied coverage of 1.64 Å (corresponding to 1.0 ML), only one site is considered. For the thicker films, starting from approximately 3 ML, when the third layer is completed, only three sites that represent the surface, the interface with W(110), and the film interior are markedly different.

The spectrum for the 1-ML coverage does not exhibit a distinct quantum beat pattern, which is in agreement with the literature data where the Curie temperature of the ML is approximately 230 K (Ref. 2). The spectrum can be fitted by a single paramagnetic component. When the nominal coverage is increased to 1.25 ML and subsequently to 1.50 ML, the measured time spectra still do not exhibit any clear indication of the onset of a long-range magnetic order. A slow beat structure has its origin in a quadrupole interaction.[41] This observation remains in agreement with the literature data.[17] However, the fits reveal that in addition to the uncovered psML regions, which are clearly identified as nonmagnetic sites, there are also DL areas present for this coverage range. The contribution from these DL areas is in good agreement with that expected from this nominal coverage, and their magnetic hyperfine field that is on the order of 4 T indicates the onset of ferromagnetism. It must be noted that the fits become ambiguous, especially concerning orientation of magnetic hyperfine field when $B_{hf}$ values are small, as it was for the 1.5 ML coverage.

A distinct quantum beat structure appeared in the time spectrum when the nominal Fe thickness reached 1.75 ML. The magnetic structure derived from this spectrum coincides with the morphology of the film observed using STM in Fig. 3; two types of DL areas (the first one with the homogenous out-of-plane magnetization and the second one with a tilted magnetization) coexist with the in-plane magnetized TL areas

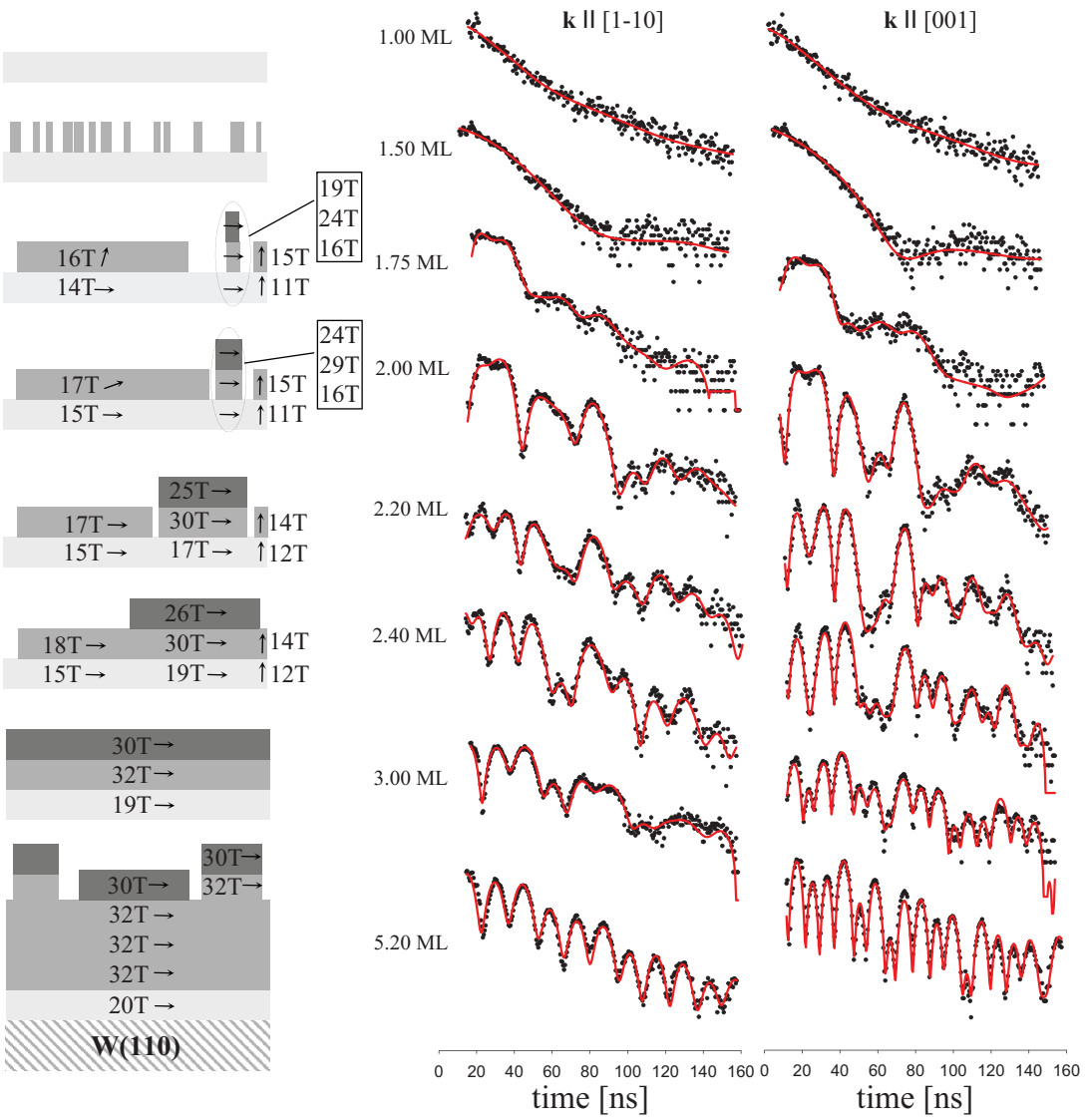


FIG. 4. (Color online) Fitted NRS time spectra of ultrathin $^{57}$Fe films on W(110) for selected (nominal) Fe coverages for $\mathbf{k_0}$ parallel to the [1-10] and [001] directions in the W(110) plane. The corresponding magnetic structures are shown. The arrows indicate the directions of the hyperfine magnetic fields, and the numbers are their magnitudes in Teslas.

and the nonmagnetic ML patches. The morphology and location of the out-of-plane magnetized DL areas is not obvious. The simplest interpretation of this result involves small separated DL patches, and many of these patches are observed in the STM image. However, an inhomogeneous magnetization distribution in the DL areas is also plausible, where the interior is magnetized in-plane and the gradual magnetization tilts to the normal at the rims of the islands. This magnetization structure could be expected if the perimeter atoms are the source of a strong perpendicular anisotropy, which was observed for cobalt islands on Pt(111).[42] The perpendicular magnetization observed in an NRS experiment for ML Fe islands on W(110) covered with silver[43] strongly supports the above picture. The derived perpendicular magnetic anisotropy of our DL areas is in agreement with the results of the low-temperature SP-STS measurements showing the out-of-plane stripe domains for DL with the linear misfit dislocations induced by growth[23] or annealing[25] at elevated temperatures.

The third AL, which begins to develop at the coverage of 1.75 ML, forces the magnetization in the TL areas into the film plane, and with increasing coverage, as the TL and thicker areas expand, the in-plane magnetic anisotropy becomes dominant. Finally, for coverages greater than 3 ML, a uniform magnetization orientation along the [1-10] direction is clearly observed from the NRS spectra, and the [1-10] direction remains the easy axis until a subsequent complex SRT to the [001] bulk easy direction occurs at 30 ML through a noncollinear magnetization structure.[31] The $B_{hf}$ value across the films remains constant (32 T) and similar to the bulk value, with the exception of the surface, where it is slightly reduced to 30 T in agreement with the CEMS results,[44] and the interface with tungsten, where it has a characteristically low value close to 20 T.[45]

## V. DISCUSSION AND COMPARISON WITH EXISTING LITERATURE DATA

It is interesting to compare our results with the available literature data on uncovered Fe/W(110), especially concerning the magnetic anisotropy of the DL areas. The bottom AL is magnetized in the sample plane along the [1-10] direction, which is consistent with the symmetry of the in-plane magnetic anisotropy for thin iron films on W(110). The second AL apparently prefers a canted magnetic state (as measured from the sample normal), where the canting angle increases from 20 degrees and finally becomes collinear with the magnetization of the bottom layer with increasing coverage at 2.2 ML. This result should be discussed in the context of the reported in-plane magnetic anisotropy of the extended DL areas at temperatures $>165$ K (Refs. 17 and 46). In this paper, we show that although in-plane magnetization dominates at RT, there is also a significant perpendicularly magnetized contribution in the DL areas that is manifested in both the noncollinear magnetic structure deduced for the large DL areas and in the out-of-plane magnetized small DL regions. The contradiction with the TOM[17]- and MOKE[46]-based results can be explained by the high local sensitivity of the NRS technique to the orientations of the magnetic moments.

However, the observation of RT out-of-plane magnetic components in the discussed coverage range is consistent with the results presented by Durkop *et al.*[21] They concluded that, in the initial state (free from adsorption effects), the DL areas are magnetized perpendicularly and that exposure of approximately 1 L is sufficient to rotate the easy direction of magnetization to the in-plane [1-10] direction (final state). They also reported that the magnetic moments in the initial and final states considerably differ, from 40% to 100% of the bulk value, respectively. The authors were unable to provide an explanation for this striking anisotropy of the magnetic moment in the DL areas. However, as a possible explanation of their TOM measurements, they indicated a noncollinear magnetization structure in the initial state, which resulted in an apparent underestimation of the value for the extracted magnetic moment.

In this context, the interpretation of our $B_{hf}$ data in terms of the local magnetization (magnetic moments) becomes crucial. This interpretation becomes possible using $B_{hf}$ versus $\mu$ cross-correlations derived from our DFT calculations performed with the WIEN2K program package. As a reference, calculations for bulk iron, approximated by the central layer of a 7-ML Fe slab, and the Fe(110) surface were performed. For metallic $\alpha$-Fe, our results are in good agreement with the established theoretical standards,[37,39] yielding $\mu = 2.25\ \mu_B$ and $B_{hf} = 35.2$ T. For the Fe(110) surface, we observed that the strong enhancement of the magnetic moment ($\mu = 2.8\ \mu_B$) contrasted with a reduction of the hyperfine magnetic field ($B_{hf} = 30$ T), which is similar to theoretical[37] and experimental[44,47] data reported in the literature. Note that the calculations only consider the Fermi contact term to $B_{hf}$, and especially for surfaces and interfaces, a dipolar contribution from orbital moment may become important.[26] When comparing the theoretical results with the experimental data, one also has to remember that the theoretical results refer to 0 K, whereas the experiment was performed at RT, which is close to the Curie temperature for the ultrathin films.

With these reservations, the calculations well interpret the experimentally observed trends, and they help to understand the magnetic properties observed by the hyperfine magnetic fields. The available experimental and theoretical results are summarized in Table I. In the 2-ML coverage of Fe on W(110), we determined $B_{hf}$ to be equal to 21 and 23 T for the first (interface) and second (surface) ALs, respectively. The experimental values, 15 and 17 T, respectively, which are significantly lower due to temperature effects, exhibit a similar trend. Therefore, by considering the corresponding values of the calculated magnetic moments, 2.25 and 2.90 $\mu_B$, respectively, which are in fair agreement with previous calculations,[26,48,49] a strong enhancement of the surface magnetic moment that amounts to more than 25% becomes evident.

Our model can also be compared to the CEMS studies for Ag covered Fe/W(110) films by Przybylski *et al.*[8] From our NRS measurements, we were able to observe significant deviations from the *a priori* assumed in Ref. 8 perfect layer-by-layer growth mode, and we were also able to resolve the number of components that arise from the partially filled ALs. Although information on the hyperfine magnetic field orientations was not accessible in the CEMS investigations, both experiments provided similar information on the layer-resolved $B_{hf}$ values, with the exception of the surface one. This result can be explained by the influence of the Ag covering layer, which partially restores translational symmetry that results in an increase of $B_{hf}$, which is in agreement with the calculations performed by Freeman *et al.*[26]

Finally, we conclude that our study sheds new light on the previous[17,21,46] results concerning the magnetization structure in ultrathin Fe films on W(110), especially concerning the SRT and the interpretation of the magnetic anisotropy in

TABLE I. Experimentally and theoretically determined magnetic moments ($\mu$) and magnetic hyperfine fields ($B_{hf}$) for Fe(110)/W(110) films. The magnetic hyperfine fields extracted from the NRS measurements are compared to results for the Ag covered Fe/W(110) films.[8] Uncertainties of the fitted $B_{hf}$ are of the order of 0.5 T.

| | | Theory (0 K) | | Experiment (300 K) | |
|---|---|---|---|---|---|
| | | Present work | Refs. 26 and 49 | Present work | Ref. 8 |
| Interface AL in DL of Fe/W(110) | $\mu$ | 2.25 $\mu_B$ | 2.30 $\mu_B$ | | |
| | $B_{hf}$ | 21 T | | 15 T | 18 T |
| Surface AL in DL of Fe/W(110) | $\mu$ | 2.90 $\mu_B$ | 2.91 $\mu_B$ | | |
| | $B_{hf}$ | 23 T | | 17 T | 27 T |

the DL. We undoubtedly proved the RT existence of the out-of-plane magnetization components in the DL areas, and we demonstrated that even the magnetic polarization effects from the in-plane magnetized TL areas do not fully destroy this scenario.

## VI. CONCLUSIONS

In conclusion, using nuclear resonant scattering of synchrotron radiation, we investigated the thickness-induced spin reorientation transition in ultrathin Fe/W(110) films in detail. During growth of the films, the magnetic state of the Fe film changes from the noncollinear configuration with the [110] out-of-plane magnetic component to the homogeneously magnetized state with the in-plane [1-10] easy direction. Our results reveal the complex character of this transition, which has been intensively studied in the past. The extremely fast acquisition of the experimental NRS spectra combined with the high sensitivity of the NRS technique to the orientation of the magnetic hyperfine fields allowed us to study magnetic evolution during the SRT in detail. The noncollinear magnetic structure appears in the system of the ML, DL, and TL areas that coexist due to the deviation from the layer-by-layer growth mode of iron on W(110). We also report on the observation of out-of-plane magnetic anisotropy in the DL areas at temperature as high as 300 K.

## ACKNOWLEDGMENTS

This work was supported in part by the Polish Ministry of Science and Higher Education and its grants for Scientific Research, by the Team Program of the Foundation for Polish Science cofinanced from the EU European Regional Development Fund, and by the Polish-French program Polonium. Calculations have been performed in the ACK Cyfronet AGH, computational Grant No. MNiSW/IBM_BC_HS21/AGH/035/2007.

*Corresponding author: mislezak@agh.edu.pl

†Present address: National Synchrotron Radiation Centre SOLARIS Jagiellonian University ul. Gronostajowa 7/P.1.6, 30-387 Kraków, Poland.

‡Present address: Institute for Synchrotron Radiation, Karlsruhe Institute of Technology, Campus Nord, 76344 Eggenstein-Leopoldshafen, Germany.

[1] C. A. F. Vaz, J. A. C. Bland, and G. Lauhoff, Rep. Prog. Phys. **71**, 056501 (2008).

[2] H. J. Elmers, J. Hauschild, H. Hoche, U. Gradmann, H. Bethge, D. Heuer, and U. Köhler, Phys. Rev. Lett. **73**, 898 (1994).

[3] O. Pietzsch, A. Kubetzka, M. Bode, and R. Wiesendanger, Phys. Rev. Lett. **84**, 5212 (2000).

[4] L. Lu, J. Bansmann, and K. H. J. Meiwes-Broer, J. Phys.: Condens. Matter **10**, 2873 (1998).

[5] D. Sander, A. Enders, C. Schmidthals, D. Reuter, and J. Kirschner, Surf. Sci. **402-404**, 351 (1998).

[6] H. J. Elmers, J. Hauschild, and U. Gradmann, Phys. Rev. B **59**, 3688 (1999).

[7] M. Przybylski, J. Korecki, and U. Gradmann, Appl. Phys. A **52**, 33 (1991).

[8] M. Przybylski, I. Kaufmann, and U. Gradmann, Phys. Rev. B **40**, 8631 (1989).

[9] D. Li, M. Freitag, J. Pearson, Z. Q. Qiu, and S. D. Bader, Phys. Rev. Lett. **72**, 3112 (1994).

[10] Z. Q. Qiu, J. Pearson, and S. D. Bader, Phys. Rev. Lett. **70**, 1006 (1993).

[11] W. Dürr, M. Taborelli, O. Paul, R. Germar, W. Gudat, D. Pescia, and M. Landolt, Phys. Rev. Lett. **62**, 206 (1989).

[12] K. Nakamura, T. Akiyama, T. Ito, and A. J. Freeman, J. Appl. Phys. **105**, 07C304 (2009).

[13] K. Nakamura, N. Mizuno, T. Akiyama, T. Ito, and A. J. Freeman, J. Appl. Phys. **101**, 09G521 (2007).

[14] N. Mizuno, K. Nakamura, T. Akiyama, and T. Ito, J. Phys.: Condens. Matter **19**, 365222 (2007).

[15] M. Przybylski and U. Gradmann, Phys. Rev. Lett. **59**, 1152 (1987).

[16] W. Weber, D. Kerkmann, D. Pescia, D. A. Wesner, and G. Güntherodt, Phys. Rev. Lett. **65**, 2058 (1990).

[17] H. J. Elmers, J. Hauschild, H. Fritzsche, G. Liu, U. Gradmann, and U. Köhler, Phys. Rev. Lett. **75**, 2031 (1995).

[18] R. Skomski, D. Sander, A. Enders, and J. Kirschner, IEEE Trans. Magn. **32**, 4567 (1996).

[19] H. J. Elmers, J. Hauschild, and U. Gradmann, Phys. Rev. B **54**, 15224 (1996).

[20] N. Weber, K. Wagner, H. J. Elmers, J. Hauschild, and U. Gradmann, Phys. Rev. B **55**, 14121 (1997).

[21] H. Durkop, H. J. Elmers, and U. Gradmann, J. Magn. Magn. Mater. **172**, L1 (1997).

[22] A. Kubetzka, O. Pietzsch, M. Bode, and R. Wiesendanger, Phys. Rev. B **63**, 140407 (2001).

[23] M. Bode, K. von Bergmann, O. Pietzsch, A. Kubetzka, and R. Wiesendanger, J. Magn. Magn. Mater. **304**, 1 (2006).

[24] R. Röhlsberger, *Nuclear Condensed Matter Physics with Synchrotron Radiation*, STMP 208 (Springer-Verlag, Berlin, 2004).

[25] S. Meckler, N. Mikuszeit, A. Preßler, E. Y. Vedmedenko, O. Pietzsch, and R. Wiesendanger, Phys. Rev. Lett. **103**, 157201 (2009).

[26] S. C. Hong, A. J. Freeman, and C. L. Fu, Phys. Rev. B **38**, 12156 (1988).

[27] S. Stankov, R. Rüffer, M. Sladecek, M. Rennhofer, B. Sepiol, G. Vogl, N.Spiridis, T. Ślęzak, and J. Korecki, Rev. Sci. Instrum. **79**, 045108 (2008).

[28] R. Rüffer and A. I. Chumakov, Hyperfine Interact. **97–98**, 589 (1996).

[29] R. Röhlsberger, Hyperfine Interact. **123–124**, 301 (1999).

[30] R. Rüffer, Hyperfine Interact. **141–142**, 83 (2002).

[31] T. Ślęzak, M. Ślęzak, M. Zając, K. Freindl, A. Kozioł-Rachwał, K. Matlak, N. Spiridis, D. Wilgocka-Ślęzak, E. Partyka-Jankowska, M. Rennhofer, A. I. Chumakov, S. Stankov, R. Rüffer, and J. Korecki, Phys. Rev. Lett. **105**, 027206 (2010).

[32] S. Couet, Th. Diederich, S. Stankov, K. Schlage, T. Ślęzak, R. Rüffer, J. Korecki, and R. Röhlsberger, Appl. Phys. Lett. **94**, 162501 (2009).

[33] S. Stankov, R. Röhlsberger, T. Ślęzak, M. Sladecek, B. Sepiol, G. Vogl, A. I. Chumakov, R. Rüffer, N. Spiridis, J. Łażewski, K. Parliński, and J. Korecki, Phys. Rev. Lett. **99**, 185501 (2007).

[34]W. Sturhahn, Hyperfine Interact. **125**, 149 (2000).
[35]X. Qian and W. Hübner, Phys. Rev. B **67**, 184414 (2003).
[36]D. Spisak and J. Hafner, Phys. Rev. B **70**, 195426 (2004).
[37]C. L. Fu and A. J. Freeman, J. Magn. Magn. Mater. **69**, L1 (1987).
[38]S. Ohnishi, A. J. Freeman, and M. Weinert, Phys. Rev. B **28**, 6741 (1983).
[39]B. Lindsen and J. Sjöström, J. Phys. F **18**, 1563 (1988).
[40]H. Bethge, D. Heuer, Ch. Jensen, K. Reshöft, and U. Köhler, Surf. Sci. **331–333**, 878 (1995).
[41]E. Partyka-Jankowska, B. Sepiol, M. Sladecek, D. Kmiec, J. Korecki, T. Ślęzak, M Zając, S. Stankov, R. Rüffer, and G. Vogl, Surf. Sci. **602**, 1453 (2008).
[42]S. Rusponi, T. Cren, N. Weiss, M. Epple, P. Buluschek, L. Claude, and H. Brune, Nat. Mater. **2**, 546 (2003).
[43]R. Röhlsberger, J. Bansmann, V. Senz, K. L. Jonas, A. Bettac, O. Leupold, R. Rüffer, E. Burkel, and K. H. Meiwes-Broer, Phys. Rev. Lett. **86**, 5597 (2001).
[44]J. Korecki and U. Gradmann, Phys. Rev. Lett. **55**, 2491 (1985).
[45]M. Przybylski, U. Gradmann, and J. Korecki, J. Magn. Magn. Mater. **69**, 199 (1987).
[46]D. Sander, R. Skomski, C. Schmidthals, A. Enders, and J. Kirschner, Phys. Rev. Lett. **77**, 2566 (1996).
[47]T. Ślęzak, J. Łażewski, S. Stankov, K. Parlinski, R. Reitinger, M. Rennhofer, R. Rüffer, B. Sepiol, M. Ślęzak, N. Spiridis, M. Zając, A. I. Chumakov, and J. Korecki, Phys. Rev. Lett. **99**, 066103 (2007).
[48]I. Galanakis, M. Alouani, and H. Dreysse, Phys. Rev. B **62**, 3923 (2000).
[49]A. J. Freeman and C. L. Fu, J. Appl. Phys. **61**, 3356 (1987).